Physics Letters A 453 (2022) 128484

Contents lists available at ScienceDirect

Physics Letters A

www.elsevier.com/locate/pla

Quantum sensing with sub-Planck structures for the dynamics of Bose-Einstein condensate in presence of engineered potential barriers inside a harmonic trap

Jayanta Bera [a], Barun Halder [b], Suranjana Ghosh [c], Ray-Kuang Lee [d,e], Utpal Roy [b,*]

[a] Department of Physics, C. V. Raman Global University, Odisha-752054, India
[b] Department of Physics, Indian Institute of Technology Patna, Patna-801106, India
[c] Indian Institute of Science Education and Research Kolkata, West Bengal-741246, India
[d] Institute of Photonics Technologies, National Tsing-Hua University, Hsinchu, Taiwan
[e] Physics Division, National Center for Theoretical Sciences, Taipei 10617, Taiwan

ARTICLE INFO

Article history:
Received 13 July 2022
Received in revised form 30 September 2022
Accepted 3 October 2022
Available online 5 October 2022
Communicated by B. Malomed

Keywords:
Bose-Einstein condensate
Quantum metrology
Sub-Planck structures

ABSTRACT

We report a scheme for quantum sensing in ultracold atoms by utilizing an atom-interferometer producing sub-Planck scale structures. The condensate is trapped in a hybrid potential, comprising of an overall harmonic trap and sharp potential barriers which are designed as 50-50 atomic beam-splitters. A scaling law for quantum sensing is established for ultracold atoms and the maximum limit of quantum sensing is identified. Quantum sensing for position, momentum and temperature are demonstrated with a sufficiently stable condensate. The present scheme reveals maximum limit of quantum sensitivity for ultracold atoms against infinitesimal external perturbations. With a designable time sequence for the trapping potential, our results provide a promising scheme for quantum sensing with Bose-Einstein condensate in atomic chips.

1. Introduction

It is well-known that interference structures are the central constituent of quantum sensing. Mesoscopic quantum superposition structures can manifest phase-space area much smaller than Planck's constant and thereby named as sub-Planck scale structures. It was first conjectured by Zurek [1] that these structures are physically meaningful and set the limit of quantum sensitivity beyond Heisenberg limit. Mesoscopic states like Schrödinger cat-state, compass-state and their generalizations are extensively studied in different physical contexts [2–9]. Underlying sub-Planck scale structures hold the secrets for developing quantum technologies through quantum precision measurements [10–18]. Some recent experimental advancements are quite intriguing to observe such effects [19–22].

On the other hand, Bose-Einstein condensate (BEC), being a long lived, coherent matter-wave of ultracold atoms, has become a promising candidate to explore various quantum mechanical phenomena [23–32]. With the development of atomic chip, matter-wave interferometry with BECs provides us an important tool for experiments in fundamental and applied physics [33]. Specially, quantum sensing is a highly emerging field for ultracold atoms in recent time [34–39]. However, without referring atomic waveguide structures, how to utilize the dynamics of a cold atomic cloud trapped in a confined potential is an important component of an atomic interferometer [40,41].

Here, we consider a model of quasi-1D BEC in presence of a hybrid trap, prepared for its optical analogue, to investigate the phase space quantum interference structures. Definite steps are proposed to show that these structures are having sub-Planck dimensions. A scaling law is established for BEC to device a connection between these interference structures with the limit of precision measurements in BEC. Though, the presence scheme is illustrated for a particular physical scenario, it will enable quantum precision measurements for a wide variety of experimental situations in this highly tunable system via trap engineering or nonlinearity management. We exploit the phenomena of tunneling and reflection (TR) of well-localized solution of an experimentally viable system of trapped ultracold atoms [42]. While studying the dynamics of a nonlinear quantum system, it is always preferable to have a non-decaying, self-similar solution like soliton [43–46]. In BEC, stable solitary wave excitations emerge from the solutions of the reduced Gross Pitäevskii equation (GPE) [47]. The observations of bright [48–54] and dark [55] solitary excitations in BEC drive intense re-

* Corresponding author.
E-mail address: uroy@iitp.ac.in (U. Roy).

https://doi.org/10.1016/j.physleta.2022.128484
0375-9601/

searches on TR [56–63]. TR in BEC are studied against a variety of potential barriers, such as Gaussian potential, Rosen-Morse potential and δ-potential [64–72]. A properly designed potential barrier can behave like an atomic beam-splitter which splits the condensate into fragments upon TR [67,73,74].

Particularly, we have considered the system of experimentally observed bright solitary wave in trapped quasi-1D BEC. The initial harmonic trap is modified by adding time-dependent sharp potential barriers, which are designed as 50-50 atomic beam-splitters. The knowledge of the positions and momenta of the bifurcated condensates are acquired by evaluating the Wigner quasi-probability phase-space distribution function, which is widely studied to manifest negative regions in phase space for nonlocal quantum superposition [75]. We investigate the formation mechanism of mesoscopic states and provide the mechanism for estimating the sensitivity to pave a suitable ground for quantum sensing applications. Sub-Planck structures and their scaling law are illustrated in our proposed scheme, with the variation of classical action with the nonlinearity. Applications as quantum sensing for position, momentum, and temperature are explored with trapped ultracold atoms. By utilizing trapping potentials with a designable time sequence, our results provide a promising scheme for quantum sensing with atomic chips.

The paper is organized as follows. In the following section, we start by solving the GPE for a cigar-shaped BEC, undergoing tunneling and reflection by properly designed atomic beam splitters. After delineating spatio-temporal behavior of the dynamics, we provide a phase-space analysis with experimental parameters in Sec. 3. A scaling law, which is important for quantum sensing, is identified for BEC and proven. We also compute the area of the phase-space structures which signify the sensitivity limit. In Sec. 4, we illustrate few physical situations for quantum precision measurements of position, momentum and temperature. We conclude in Sec. 5 after pointing out some additional aspects.

2. Dynamics of the condensate with tunneling and reflection

It is now worthwhile to identify the physical situation and investigate the dynamics, which is governed by the well-known GPE [76]. Under an asymmetric harmonic trap ($\omega_r = \omega_y = \omega_z \gg \omega_x$), the condensate is known to manifest a cigar-shaped scenario. The dynamics of a cigar-shaped BEC, composed of N atoms of each mass M, and transverse harmonic oscillator length $l_r = \sqrt{\hbar/M\omega_r}$ is represented by [77]

$$i\hbar\frac{\partial\psi(x,t)}{\partial t} = \Big[-\frac{\hbar^2}{2M}\frac{\partial^2}{\partial x^2} + \frac{M}{2}\omega_x^2 x^2 + 2N\hbar\omega_r a|\psi(x,t)|^2\Big]\psi(x,t), \tag{1}$$

where a is the s-wave scattering length. It is convenient to reduce the above equation to a dimensionless form by scaling position, time and energy with l_r, $1/\omega_r$ and $\hbar\omega_r$, respectively [78].

$$i\frac{\partial\psi(x,t)}{\partial t} = \Big[-\frac{1}{2}\frac{\partial^2}{\partial x^2} + \frac{1}{2}\nu_x^2 x^2 + g_{1d}|\psi(x,t)|^2\Big]\psi(x,t), \tag{2}$$

where the nonlinearity coefficient is $g_{1d} = 2N(a/l_r)$ and $\nu_x = \omega_x/\omega_r$. The condensate is confined in a harmonic trap and made to collide with a sharp Gaussian barrier: $v_T(t,x) = v_0(t)exp[-(x - d_0(t))^2/(2\sigma^2)]$ [61], which can be created and controlled by a far blue-detuned laser beam [39,79]. The resultant potential takes the form

$$v_{ext}(x,t) = \tfrac{1}{2}\nu_x^2 x^2 + v_T(t,x). \tag{3}$$

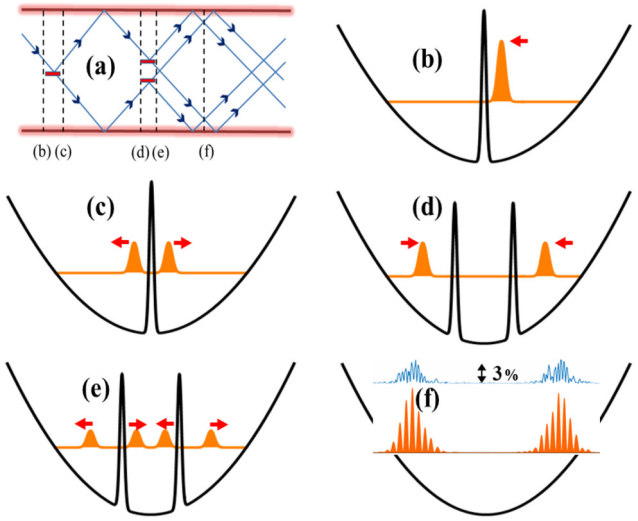

Fig. 1. (a) A schematic representation of the optical analogue of the dynamics where the potential barriers are replaced by beam-splitters. Time instances for showing the density patterns are designated by dashed lines (b-f) in (a). In figures (b)-(f), condensate densities are shown by filled-plots and traps are drawn by dark-lines. Arrows beside the densities are to indicate the directions of motion of the condensates at that time. Figures (b) and (c) depict the densities before and after the collision with the first beam-splitter, where as figures (d) and (e) are the same after the collisions by the pair of second beam-splitters, respectively. Figure (f) shows density pattern at time $t = 13.1$ ms, for which the stability analysis is also carried out by displaying the percentage deviation in the inset.

We have used all the parameters dimensionless throughout this work unless mentioned otherwise. For investigating the condensate dynamics, we solve 1D-GPE (Eq. (2)) by Fourier split-step method [80]. The spatial coordinate is divided into 10×2^8 grids with step-size 0.15 and time is divided into 5000 grids with time-step 0.02. Numerical computation was performed in a blade-server: processor-Intel Xeon CPU $E5640$ @ 2.67 GHz, RAM-64 GB, having 30 minutes as the single run-time. For illustrating our results, we consider experimental parameters for ${}^7_3Li$: $M = 7$ a.u., $N = 6 \times 10^3$, $\omega_r = 2\pi \times 710$ Hz, $l_r = 1.4257$ µm, $a = -0.21$ nm, $g_{1d} = -1.767$ and $\nu_x = 0.0986$ [48]. The condensate is loaded with higher energy inside the harmonic trap to observe density oscillation of larger amplitude [53,67]. The initial condensate is taken as a Gaussian with waist 2.138 µm and distance from origin, 42.76 µm. Upon collision with the barrier, the coherent cloud breaks into two parts (tunneling and reflection) [53]. Condensate densities along with the potential profiles at different times are displayed in Fig. 1. The whole dynamics is represented through an optical analogue (Fig. 1 (a)), where time-instances for observations are marked by dashed-lines (b-f) in Fig. 1 (a). Condensate densities are shown by filled-plots. Figs. 1 (b) and (c) depict the densities before and after the interaction with the first beam-splitter, whereas Fig. 1 (d) and (e) are the same after the interactions by the pair of second beam-splitters, respectively. Condensate experiences first collision at $t = 3.36$ ms and second collisions at $t = 9.60$ ms. Post first collision, the daughter clouds move with opposite velocities till they turn back in the course of oscillation inside the trap. They collide again with two barriers, which results into four fragments as shown in Fig. 1 (e).

Stability Check: For checking the numerical stability of the chosen condensate wavefunction, we choose a time ($t = 13.1$ ms), when the condensate reveals only two symmetrically placed interference oscillations in coordinate space (Fig. 1(f)). We choose this structure for presenting the stability analysis because a stable oscillating interference structure (percentage deviation below 3%) at higher time will undoubtedly confirm the stability at any time prior to that. The said numerical stability analysis is performed by

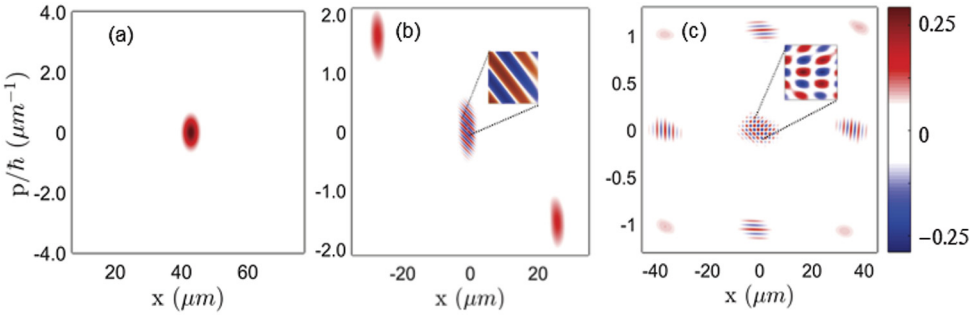

Fig. 2. Wigner distribution of (a) the initial cloud, (b) Schrödinger cat state produced at 9.18 ms, and (c) compass-like state of north-north-south-south type at 13.1 ms. (For interpretation of the colors in the figure(s), the reader is referred to the web version of this article.)

Table 1
The condensate fractions after the first collision are denoted by c_1 and c_2 at $t = 9.18$ ms (the dashed line (c) in Fig. 1 (a)). The four fractions after the second set of collisions are denoted by c_3, c_4, c_5 and c_6 at $t = 11.2$ ms (the dashed line (e) in Fig. 1 (a)). Set-II is the desired model for 50-50 beam-splitters with equally distributed condensate fractions.

Parameter sets	1^{st} Observation ($t = 9.18$ ms)		2^{nd} Observation ($t = 11.20$ ms)			
–	c_1	c_2	c_3	c_4	c_5	c_6
Set-I	0.578	0.422	0.237	0.249	0.331	0.183
Set-II	0.505	0.495	0.24	0.256	0.26	0.242
Set-III	0.446	0.554	0.235	0.256	0.213	0.295

adding a random noise to the initial wave function. The maximum value of the noise is taken 5% of the peak value. The noisy wave function evolves with time and is compared with the exact result after 13.10 ms by depicting the deviation in Fig. 1(f).

Condensate fractions after collision primarily depend on $v_0(t)$, $d_0(t)$, and σ [81]. A proper tuning of these parameters can lead to equal condensate fractions in both parts post-collision and the device becomes analogous to a 50-50 atomic beam-splitter [67,82]. Different sets of these parameters are tested and presented in Table-1 for $\sigma = 0.285$ μm. For the first beam-splitter, $v_0(t)$ takes values $5.51\hbar\omega_r$, $6.05\hbar\omega_r$, and $6.51\hbar\omega_r$ for set-I, set-II and set-III, respectively. It is apparent that an approximate 50-50 atomic beam-splitter is obtained for set-II ($v_0(t) = 6.05\hbar\omega_r$). For the second collision with the pair of beam-splitters, $v_0(t)$'s are taken as 0.73 and 0.85 times the first case for all the sets in Table-1. These values are taken as per the instantaneous values of the density just prior to the collisions. We have chosen set-II, where c_1 and c_2 are of equal fractions after splitting and c_3, c_4, c_5 and c_6 are almost of one-fourth fractions each, giving us a desired situation to investigate.

3. Sub-Planck scale structures and scaling law

A phase-space analysis is conducive to investigate the quantum interference structures of the condensate fragments. The Wigner quasi-probability distribution function,

$$W(x,p) = \frac{1}{\pi\hbar}\int_{-\infty}^{\infty} \psi^*(x+q,t)\psi(x-q,t)e^{2ipq/\hbar}dq, \tag{4}$$

are delineated in Fig. 2 at different times. The condensate is initially placed at a distance 42.76 μm from the center of the trap (Fig. 2 (a)) and collides with the potential barrier of amplitude $v_0(t) = 6.05\hbar\omega_r$ after $t = 3.36$ ms [72]. Two produced daughter condensates move with opposite momentum upto the time $t = 9.6$ ms, when the second collision takes place. During this interval, the condensate is a Schrödinger cat-state, rotating in phase space with time. A time snapshot of the Wigner function at $t = 9.18$ ms is displayed in Fig. 2(b). The visibility of the interference ripples depends on the proper choice of the potential parameters as mentioned for set-II in Table 1. Subsequently, a pair of potential barriers at $d_0(t) = \pm 21.38$ μm act as 50-50 beam-splitters and each condensate fraction after collision carries one-fourth of the total density (Table 1). One will have a rotated compass-like states in phase space during the interval, 9.6 ms $\leq t \leq$ 20.1 ms. A phase-space Wigner function at time snapshot ($t = 13.1$ ms) is a symmetrically spaced compass-like state of north-north-south-south type, illustrated in Fig. 2(c). The central interference structures are highly oscillatory, produced due to the interference of two diagonal cat-states. These structures are squeezed in both position and momentum, termed as sub-Planck scale structures. The sub-Planck scale structures were first reported in a seminal paper in the year 2001 [1], where these structures were held responsible for quantum sensitivity beyond Heisenberg limit. In the following paragraph, we will explicitly show the sub-Planck behavior of these structures for ultracold atoms.

3.1. Establishing the scaling law

In order to estimate the dimension of the interference structures, we need to evolve a scheme for estimation. Our first step is to verify that the structures are very tiny and much below Planck-scale. The classical action ('A') of the state at a given time is defined as the product of the range of effective support of its state in phase-space: $A = \triangle x \times \triangle p$, where the uncertainties are calculated by standard definitions: $\triangle x = \sqrt{\langle x^2\rangle - \langle x\rangle^2}$ and $\triangle p = \sqrt{\langle p^2\rangle - \langle p\rangle^2}$. The phase-space area, 'a', of the maxima or minima tiles in the central interference region can be estimated, provided one connects it to a global system property, which is measurable. Unlike other physical systems, a scaling law between 'a' and 'A' is easy to establish for systems modeled by harmonic oscillator [1]. However, establishing an appropriate scaling law becomes mandatory for BEC before precisely estimating a. In Fig. 1, it is apparent that the trajectory and the spatial density distributions during 13.1 ms $\leq t <$ 16.6 ms is a mirror image of the density flow during 9.6 ms $\leq t <$ 13.1 ms. However, the same during 16.6 ms $\leq t <$ 20.1 ms is identical (modulo some natural decay) to that during 9.6 ms $\leq t <$ 13.1 ms. Hence, investigating any one of these parts, preferably the first time window (9.6 ms $\leq t <$ 13.1 ms) is sufficient. We choose five time instances: 9.6 ms, 11.2 ms, 12.09 ms, 12.54 ms and 13.1 ms for which the estimations of A are carried out by using the numerically computed order parameter of the condensate. The classical action ranges in between 35.96 au $\leq A \leq$ 40.4 au. The phase space area of the cross-diagonal superposition structures in compass-like state at these instances (a) are also calculated from the FWHM of the sharp peaks in the Wigner distribution plot like the one shown in Fig. 2(c) at 13.1 ms. The corresponding range of a is found as 0.28 au $\geq a \geq$ 0.245 au. These values signify very small structures (much below Planck-

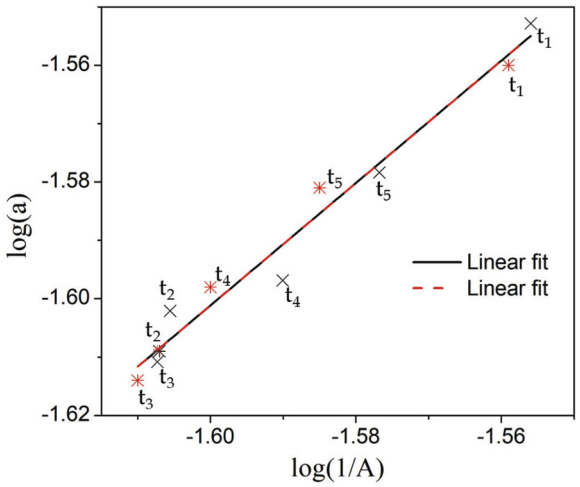

Fig. 3. Plot ($\log_e(a)$-$\log_e(1/A)$) for verifying the scaling law for two different values of nonlinearity $g_{1d} = -0.841$ ($*$) and $g_{1d} = -1.767$ ($\times$). The linear fit of the data of the first set (red line) and the second set (dashed line) provides slopes 1.04 and 1.05, respectively. The times t_1 to t_5 are 9.85 ms, 11.20 ms, 12.09 ms, 12.54 ms and 13.10 ms in sequence.

scale, *i.e.*, $a \ll 1$) and highest level of sensitivity in this system which is never reported before.

For verifying the scaling law, we plot five sets of values of A and a in Fig. 3. We have also repeated our study for two separate nonlinearities: $g_{1d} = -0.841$ and $g_{1d} = -1.767$. Both of these $\log_e - \log_e$ plots affirm an appropriate linear fit with slope approximately one, which suggest the scaling law for BEC as

$$a \sim 1/A. \tag{5}$$

This formula will now initiate a favorable way to estimate sensitivity limit against an infinitesimal change of an observable.

3.2. Variation of classical action with the nonlinearity

The size of the tiles, which is inversely proportional to the classical action (Eq. (5)), sets the limit of the sensitivity. We would like to see how the inter-atomic interactions, manifested by the attractive nonlinearity, influence the sensitivity limit. In Fig. 4, we depict the variation of the classical action with the attractive interaction at a chosen time, $t = 11.6$ ms, when the condensates has a four-way split. The classical action *vs* nonlinearity curve fits well to a line of slope -1.05 (~ -1) and hence implies inversely proportional variation. It reveals an interesting fact that a weaker attractive interaction makes the system more sensitive than a stronger one. In other words, a condensate with a weaker attractive interaction between the constituents atoms is more suitable for quantum sensing. It has been observed that the values of nonlinearity away from the range which is depicted in the figure are inappropriate to produce four-way splits and thus difficult to measure a.

4. Quantum sensing with examples

We take up couple of situations to perform quantum precision measurements of some of the observables. Let us consider an infinitesimal perturbation of the external harmonic trap, resulting into to a small spatial shift of the beam point-of-focus by an amount δ, where the strength remains unchanged. The corresponding change in kinetic energy is $(1/2)\nu_x^2\delta(2x_0 - \delta)$. It is worth recalling that any two quantum wave-functions are distinguishable provided they become orthogonal or their overlap is zero. The sensitivity limit is defined by the minimum change, which can just

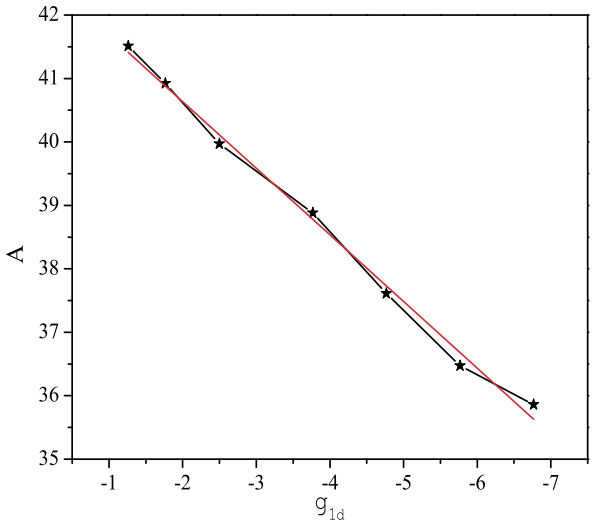

Fig. 4. The variation of classical action (A) with the attractive nonlinearity (g_{1d}). ($\star$) marked points are corresponding to the time, $t = 11.6$ ms and the red line is the linear fit of the points with slope -1.05.

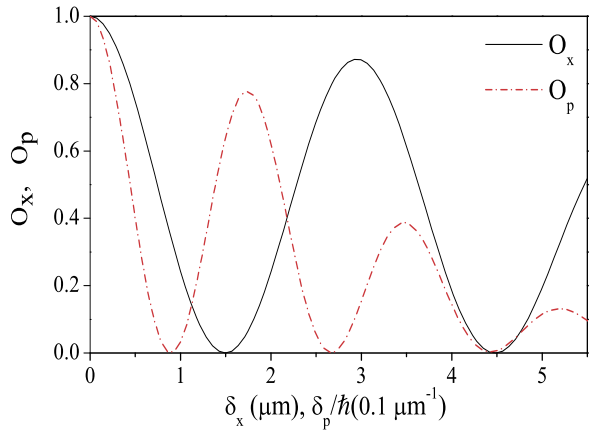

Fig. 5. The overlap functions (O_x, O_p) at $t_0 = 13.1$ ms with perturbations along x-(δ_x) and p-directions (δ_p), respectively. Zeroes of the curves are the points of orthogonality in the respective quadrature.

make the overlap integral between the initial and the perturbed wave-functions to vanish. In the context of phase-space interference structures, Wigner function, being a quasi probability distribution, is connected to the state overlap function:

$$|\langle\psi(x,t)|\psi_\delta(x,t)\rangle|^2 = \int\int W(x,p,t)W_\delta(x,p,t)dxdp, \tag{6}$$

where, $\psi_\delta(x,t)$ and $W_\delta(x,p,t)$ are the perturbed wave function and perturbed Wigner function at time t, respectively. In the following, we will illustrate quantum sensing with specific examples. Compass-like states, appearing after 9.6 ms, exhibits smallest interference structures and thus become suitable choice for quantum sensing.

4.1. Quantum sensing for position and momentum

We have illustrated the overlap functions (O_x and O_p), which are the absolute square of the scalar product between the initial and perturbed states (LHS of Eq. (6)), in both the quadratures, such that δ_x and δ_p are the values of the displacement of the compass-like state at $t = 13.1$ ms along x- and p-directions in phase space, respectively (Fig. 5). Infinitesimal perturbation which will make the perturbed state quasi-orthogonal with the initial one will make

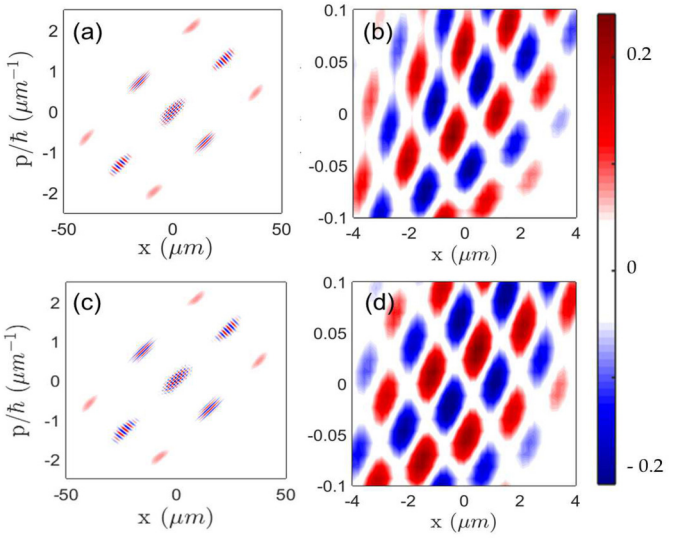

Fig. 6. Phase-space Wigner distributions of the unperturbed state (a-b) and perturbed state (c-d) at time $t_0 = 11.2$ ms. Figures (b) and (d) are the enlarged views of the central interference region, which manifest the displacement by one tile, making the states just quasi-orthogonal.

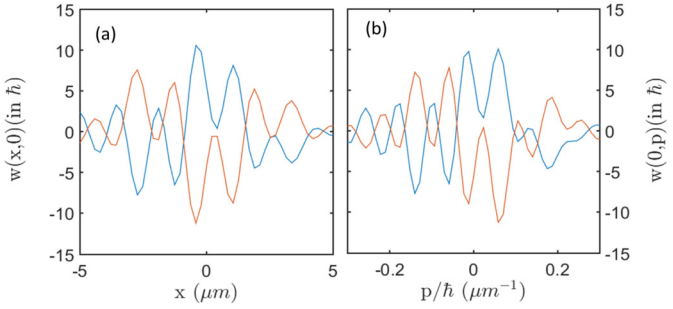

Fig. 7. Projections of the Wigner plots of Fig. 6 along x- or p-direction, by keeping the other coordinate fixed: (a) $p = 0$ and (b) $x = 0$. Red lines are for unperturbed states and blue lines are for perturbed states.

the two states distinguishable. Zeros of the overlap function in Fig. 5 are the sensitivity limit for position (1.5 μm) and momentum ($0.085\hbar$ μm^{-1}) at this time instance. These are the limits of quantum sensing at this particular time for instance. However, there may be possibilities to have other suitable times during the time-evolution with improved quantum sensing.

Let us now bring out the meaning of quantum sensing in phase-space. Fig. 6(a) depicts Wigner function of the compass-like state at time $t_0 = 11.2$ ms. We have varied different parameter values for identifying the limit of quantum sensing and finally consider a shift, $\delta = 0.31$ μm, which introduces 1.46% change in kinetic energy of the condensate. The perturbed Wigner function is depicted in Fig. 6(c), which looks as a replica of the unperturbed Wigner function (Fig. 6(a)). However, it is fascinating to observe that the numerical value of their overlap integral gave almost null result, implying that these two states are quasi-orthogonal to each other. This visualization is the sequel of Eq. (6). The elucidation lies in Fig. 6(b) and Fig. 6(d), which are the enlarged views of the central interference region of Fig. 6(a) and Fig. 6(c), respectfully. In these enlarged views, it is clearly visible that the red tiles (positive peak) are replaced by blue tiles (negative peak). Hence, one would expect a quasi-orthogonality inherent in this illustration. Projections of these two Wigner functions along x- and p-directions are shown in Fig. 7, which reveals that the state after perturbation becomes quasi-orthogonal in both the directions in phase space because their phase-space oscillations are opposite to each other.

4.2. Quantum sensing for temperature

Here, we explore the possibility of an indirect quantum precision measurement of temperature in BEC. Precise temperature estimation is always demanding but a nontrivial task. The process of thermometric measurement of temperature can be broadly categorized in two types: time of flight measurement on BEC [83–86] or impurities added on it [87–89]. Our method is entirely different from these methods and address sensitivity upto pico-Kelvin, the maximum precision of temperature estimation till date. The external perturbation could be caused by the displacement of the optical trap lens position by an amount $\delta = 0.31$ μm. The trap is created by a Gaussian laser beam of wavelength $\lambda = 532$ nm, power $P = 1.2$ mW and beam waist $w_0 = 2$ μm. The beam waist at a distance x along the direction of the beam propagation is given by $w_x = w_0\sqrt{1 + (x/x_r)^2}$, where $x_r = \pi w_0^2/\lambda$ is the Rayleigh length. The static dipole polarizability (α) of lithium is 1.6488×10^{-41} C^2 m^2 J^{-1} [90]. Hence, the trap depth (U_x) on the axis is given by

$$U_x = \frac{\alpha P}{\pi \epsilon_0 c w_x^2}, \tag{7}$$

where permittivity (ϵ_0) is 8.854×10^{-12} F/m and speed of light (c) is 3×10^8 m/s. The infinitesimal change in temperature (ΔT) is calculated from Eq. (7):

$$\Delta T = 2(U_0 - U_\delta)/K_B = 15.6 \times 10^{-12} K = 15.5\ pK, \tag{8}$$

where K_B is the Boltzmann constant. Thus, our present measurement scheme for BEC also reports a precision temperature estimation upto pico-Kelvin, which is the highest precision limit of temperature measurement to the authors' knowledge.

5. Conclusions

We have studied the dynamics of a trapped quasi-1D BEC, which experiences collisions with appropriately placed sharp potential barriers in the course of its time evolution. The considered parameters are from the first experiment of bright solitary trains in BEC. The probabilities of tunneling and reflection are properly tuned, such that the barrier potentials act like 50-50 beam-splitters. This adjustment is also required in laboratory for having maximum visibility of the interference fringes. The dynamical model is presented through a space-time plot of the condensate density. Phase-space Wigner distribution functions at varied time snapshots manifest Schrödinger cat state and compass-like state. A conducive formula relating the classical action is established for the first time in this system to quantify the dimensions of the resulting mesoscopic quantum superposition structures. The computed phase space area of the structures are much less than the Planck-limit, paving the possibility of an efficient quantum metrology beyond Heisenberg limit. We illustrate examples to create quasi-orthogonal states which can be distinguished after negligible external fluctuations. Precision measurement schemes for position, momentum and temperature are delineated. The present work can also be applied towards gravimetry and rotation sensing.

CRediT authorship contribution statement

Jayanta Bera: Writing – original draft, Visualization, Investigation, Formal analysis, Data curation. **Barun Halder:** Validation, Methodology, Investigation, Formal analysis. **Suranjana Ghosh:** Writing – review & editing, Visualization, Supervision, Methodology, Investigation, Conceptualization. **Ray-Kuang Lee:** Writing – review & editing, Methodology, Formal analysis. **Utpal Roy:** Writing

– review & editing, Writing – original draft, Visualization, Validation, Supervision, Investigation, Conceptualization.

Declaration of competing interest

The authors declare that they have no known competing financial interests or personal relationships that could have appeared to influence the work reported in this paper.

Data availability

No data was used for the research described in the article.

References

[1] W.H. Zurek, Nat. Phys. Lett. 412 (2001) 712, https://doi.org/10.1038/35089017, https://www.nature.com/articles/35089017.

[2] A. Ourjoumtsev, F. Ferreyrol, R. Tualle-Brouri, P. Grangier, Nat. Phys. Lett. 5 (2009) 189, https://doi.org/10.1038/nphys1199, https://www.nature.com/articles/35089017.

[3] F. Toscano, D.A.R. Dalvit, L. Davidovich, W.H. Zurek, Phys. Rev. A 73 (2006) 023803, https://doi.org/10.1103/PhysRevA.73.023803, https://link.aps.org/doi/10.1103/PhysRevA.73.023803.

[4] P. Kumar, R.K. Lee, Opt. Commun. 394 (2017) 23, https://doi.org/10.1016/j.optcom.2017.02.066.

[5] B. Vlastakis, G. Kirchmair, Z. Leghtas, S.E. Nigg, L. Frunzio, S.M. Girvin, M. Mirrahimi, M.H. Devoret, R.J. Schoelkopf, Science 342 (2013) 607, https://doi.org/10.1126/science.1243289, https://pubmed.ncbi.nlm.nih.gov/24072821/.

[6] S. Ghosh, A. Chiruvelli, J. Banerji, P.K. Panigrahi, Phys. Rev. A 73 (2006) 013411, https://doi.org/10.1103/PhysRevA.73.013411, https://link.aps.org/doi/10.1103/PhysRevA.73.013411.

[7] U. Roy, S. Ghosh, P.K. Panigrahi, D. Vitali, Phys. Rev. A 80 (2009) 052115, https://doi.org/10.1103/PhysRevA.80.052115, https://link.aps.org/doi/10.1103/PhysRevA.80.052115.

[8] S. Ghosh, I. Manzoli, Int. J. Quantum Inf. 09 (2011) 1519, https://doi.org/10.1142/S0219749911008155, https://www.worldscientific.com/doi/epdf/10.1142/S0219749911008155.

[9] L. Praxmeyer, P. Yang, R.K. Lee, Phys. Rev. A 93 (2016) 042122, https://doi.org/10.1103/PhysRevA.93.042122, https://link.aps.org/doi/10.1103/PhysRevA.93.042122.

[10] S. Ghosh, U. Roy, C. Genes, D. Vitali, Phys. Rev. A 79 (2009) 052104, https://doi.org/10.1103/PhysRevA.79.052104, https://link.aps.org/doi/10.1103/PhysRevA.79.052104.

[11] S. Ghosh, Int. J. Quantum Inf. 10 (2012) 1250014, https://doi.org/10.1142/S0219749912500141, https://www.worldscientific.com/doi/abs/10.1142/S0219749912500141.

[12] S. Ghosh, U. Roy, Phys. Rev. A 90 (2014) 022113, https://doi.org/10.1103/PhysRevA.90.022113, https://link.aps.org/doi/10.1103/PhysRevA.79.052104.

[13] S. Ghosh, R. Sharma, U. Roy, P.K. Panigrahi, Phys. Rev. A 92 (2015) 053819, https://doi.org/10.1103/PhysRevA.92.053819, https://link.aps.org/doi/10.1103/PhysRevA.92.053819.

[14] S. Ghosh, J. Bera, P.K. Panigrahi, U. Roy, Int. J. Quantum Inf. 17 (2019) 1950019, https://doi.org/10.1142/S0219749919500199, https://www.worldscientific.com/doi/abs/10.1142/S0219749919500199.

[15] M. Stobińska, G.J. Milburn, K. Wódkiewicz, Phys. Rev. A 78 (2008) 013810, https://doi.org/10.1103/PhysRevA.78.013810, https://link.aps.org/doi/10.1103/PhysRevA.78.013810.

[16] M. Rohith, C. Sudheesh, Phys. Rev. A 92 (2015) 053828, https://doi.org/10.1103/PhysRevA.92.053828, https://link.aps.org/doi/10.1103/PhysRevA.92.053828.

[17] S. Bose, K. Jacobs, P.L. Knight, Phys. Rev. A 56 (1997) 4175, https://doi.org/10.1103/PhysRevA.56.4175, https://link.aps.org/doi/10.1103/PhysRevA.56.4175.

[18] G.S. Agarwal, P.K. Pathak, Phys. Rev. A 70 (2004) 053813, https://doi.org/10.1103/PhysRevA.70.053813, https://link.aps.org/doi/10.1103/PhysRevA.70.053813.

[19] E.V. Mikheev, A.S. Pugin, D.A. Kuts, S.A. Podoshvedov, N.B. An, Sci. Rep. 9 (2019) 14301.

[20] J. Hastrup, J.S. Neergaard-Nielsen, U.L. Andersen, Opt. Lett. 45 (2020) 640–643.

[21] J. Rivera-Dean, Th. Lamprou, E. Pisanty, P. Stammer, A.F. Ordóñez, A.S. Maxwell, M.F. Ciappina, M. Lewenstein, P. Tzallas, Phys. Rev. A 105 (2022) 033714.

[22] G.S. Thekkadath, B.A. Bell, I.A. Walmsley, A.I. Lvovsky, Quantum 4 (2020) 239.

[23] O. Morizot, Y. Colombe, V. Lorent, H. Perrin, B.M. Garraway, Phys. Rev. A 74 (2006) 023617.

[24] J. Bera, S. Ghosh, L. Salasnich, U. Roy, Phys. Rev. A 102 (2020) 063323.

[25] S.K. Giri, B. Sen, C.R. Ooi, A. Pathak, Phys. Rev. A 89 (2014) 033628.

[26] M. Takahashi, S. Ghosh, T. Mizushima, K. Machida, Phys. Rev. Lett. 98 (2007) 260403.

[27] A. Celi, A. Sanpera, V. Ahufinger, M. Lewenstein, Phys. Scr. 92 (2017) 013003, https://doi.org/10.1088/1402-4896/92/1/013003, https://link.aps.org/doi/10.1103/PhysRevA.70.053813.

[28] E.M. Wright, D.F. Walls, J.C. Garrison, Phys. Rev. Lett. 77 (1996) 2158, https://doi.org/10.1103/PhysRevLett.77.2158, https://link.aps.org/doi/10.1103/PhysRevLett.77.2158.

[29] I. Bloch, J. Dalibard, S. Nascimbène, Nat. Phys. 8 (2012) 267, https://doi.org/10.1038/nphys2259, https://www.nature.com/articles/nphys2259.pdf.

[30] A. Nath, U. Roy, Laser Phys. Lett. 11 (2014) 115501, https://doi.org/10.1088/1612-2011/11/11/115501, https://iopscience.iop.org/article/10.1088/1612-2011/11/11/115501/pdf.

[31] A. Nath, J. Bera, S. Ghosh, U. Roy, Sci. Rep. 10 (2020) 9016, https://doi.org/10.1038/s41598-020-65765-9, https://www.nature.com/articles/s41598-020-65765-9.pdf.

[32] N. Kundu, A. Nath, J. Bera, S. Ghosh, U. Roy, Phys. Lett. A 427 (2022) 127922.

[33] T. Schumm, S. Hofferberth, L.M. Andersson, S. Wildermuth, S. Groth, I. Bar-Joseph, J. Schmiedmayer, P. Kruger, Nat. Phys. 1 (2005) 57, https://doi.org/10.1038/nphys125, https://www.nature.com/articles/nphys2259.pdf.

[34] P. Berman, Atom Interferometry, Elsevier, 1996.

[35] P.A. Altin, M.T. Johnsson, V. Negnevitsky, G.R. Dennis, R.P. Anderson, J.E. Debs, S.S. Szigeti, K.S. Hardman, S. Bennetts, G.D. McDonald, New J. Phys. 15 (2013) 023009, https://doi.org/10.1088/1367-2630/15/2/023009, https://iopscience.iop.org/article/10.1088/1367-2630/15/2/023009/pdf.

[36] S. Abend, M. Gebbe, M. Gersemann, H. Ahlers, H. Müntinga, E. Giese, N. Gaaloul, C. Schubert, C. Lämmerzahl, W. Ertmer, W.P. Schleich, E.M. Rasel, Phys. Rev. Lett. 117 (2016) 203003, https://doi.org/10.1103/PhysRevLett.117.203003, https://link.aps.org/doi/10.1103/PhysRevLett.117.203003.

[37] E.R. Moan, R.A. Horne, T. Arpornthip, Z. Luo, A.J. Fallon, S.J. Ber, C.A. Sackett, Phys. Rev. Lett. 124 (2020) 120403, https://doi.org/10.1103/PhysRevLett.124.120403, https://journals.aps.org/prl/abstract/10.1103/PhysRevLett.124.120403.

[38] M.D. Lachmann, E.M. Rasel, Nat. Phys. 582 (2020) 186, https://doi.org/10.1038/d41586-020-01653-6, https://media.nature.com/original/magazine-assets/d41586-020-01653-6/d41586-020-01653-6.pdf.

[39] M.R. Andrews, C.G. Townsend, H. Miesner, D.S. Durfee, D.M. Kurn, W. Ketterle, Science 275 (1997) 637, https://doi.org/10.1126/science.275.5300.637, https://pubmed.ncbi.nlm.nih.gov/9005843/.

[40] N. Gaaloul, A. Suzor-Weiner, L. Pruvost, M. Telmini, E. Charron, Phys. Rev. A 74 (2006) 023620, https://doi.org/10.1103/PhysRevA.74.023620, https://journals.aps.org/pra/abstract/10.1103/PhysRevA.74.023620.

[41] L. Pezzé, A. Smerzi, G.P. Berman, A.R. Bishop, L.A. Collins, Phys. Rev. A 74 (2006) 023620, https://doi.org/10.1103/PhysRevA.74.033610, https://link.aps.org/doi/10.1103/PhysRevA.74.033610.

[42] C.H. Wang, T.M. Hong, R.K. Lee, D.W. Wang, Opt. Express 20 (2012) 22677, https://doi.org/10.1364/OE.20.022675, http://www.osapublishing.org/oe/abstract.cfm?URI=oe-20-20-22675.

[43] J.S. Russell, Report of the Fourteenth Meeting of the British Association for the Advancement of Science, John Murray, London, 1845.

[44] D.V. Tsarev, S.M. Arakelian, Y.-L. Chuang, R.-K. Lee, A.P. Alodjants, Opt. Express 26 (2018) 19583–19595, https://doi.org/10.1364/OE.26.019583, http://www.osapublishing.org/oe/abstract.cfm?URI=oe-26-15-19583.

[45] D.V. Tsarev, T.V. Ngo, R.K. Lee, A.P. Alodjants, New J. Phys. 21 (2019) 083041, https://doi.org/10.1088/1367-2630/ab398e, https://iopscience.iop.org/article/10.1088/1367-2630/ab398e/meta.

[46] D.V. Tsarev, A.P. Alodjants, T.V. Ngo, R.K. Lee, New J. Phys. 22 (2020) 113016, https://doi.org/10.1088/1367-2630/abc601, https://iopscience.iop.org/article/10.1088/1367-2630/abc601/meta.

[47] P. Kevrekidis, D. Frantzeskakis, R. Carretero-Gonzalez, Emergent Nonlinear Phenomena in Bose-Einstein Condensates, Springer, New York, 2008, https://carretero.sdsu.edu/publications/postscript/bec_book_cover.pdf.

[48] L. Khaykovich, F. Schreck, G. Ferrari, T. Bourdel, J. Cubizolles, L.D. Carr, Y. Castinand, C. Salomon, Science 296 (2002) 1290, https://doi.org/10.1126/science.1071021, https://www.science.org/doi/10.1126/science.1071021.

[49] K.E. Strecker, G.B. Partridge, A.G. Truscott, R.G. Hulet, Nat. Phys. 417 (2002) 150, https://doi.org/10.1038/nature747, https://pubmed.ncbi.nlm.nih.gov/11986621/.

[50] P. Medley, M.A. Minar, N.C. Cizek, D. Berryrieser, M.A. Kasevich, Phys. Rev. Lett. 112 (2014) 060401, https://doi.org/10.1103/PhysRevLett.112.060401, https://link.aps.org/doi/10.1103/PhysRevLett.112.060401.

[51] S.L. Cornish, S.T. Thompson, C.E. Wieman, Phys. Rev. Lett. 96 (2006) 170401, https://doi.org/10.1103/PhysRevLett.96.170401, https://link.aps.org/doi/10.1103/PhysRevLett.96.170401.

[52] R. Bhaduri, S. Ghosh, M. Murthy, D. Sen, J. Phys. A, Math. Gen. 34 (2001) 6553.

[53] A. Marchant, T. Billam, T. Wiles, M. Yu, S. Gardiner, S. Cornish, Nat. Commun. 4 (2013) 1865, https://doi.org/10.1103/PhysRevLett.96.170401, https://www.nature.com/articles/ncomms2893.

[54] G.D. McDonald, C.C.N. Kuhn, K.S. Hardman, S. Bennetts, P.J. Everitt, P.A. Altin, J.E. Debs, J.D. Close, N.P. Robins, Phys. Rev. Lett. 113 (2014) 013002, https://doi.org/10.1103/PhysRevLett.113.013002, https://link.aps.org/doi/10.1103/PhysRevLett.113.013002.

[55] S. Burger, K. Bongs, S. Dettmer, W. Ertmer, K. Sengstock, A. Sanpera, G.V. Shlyapnikov, M. Lewenstein, Phys. Rev. Lett. 83 (1999) 5198, https://doi.

org/10.1103/PhysRevLett.83.5198, https://link.aps.org/doi/10.1103/PhysRevLett.83.5198.
[56] M.J. Holland, L.D. Carr, B.A. Malomed, J. Phys. B, At. Mol. Opt. Phys. 38 (2005) 3217.
[57] O. Zobay, B. Garraway, Phys. Rev. A 61 (2000) 033603.
[58] A.L. Marchant, T.P. Billam, M.M.H. Yu, A. Rakonjac, J.L. Helm, J. Polo, C. Weiss, S.A. Gardiner, S.L. Cornish, Phys. Rev. A 93 (2016) 021604, https://doi.org/10.1103/PhysRevA.93.021604, https://link.aps.org/doi/10.1103/PhysRevA.93.021604.
[59] H. Sakaguchi, B.A. Malomed, New J. Phys. 18 (2016) 025020, https://doi.org/10.1088/1367-2630/18/2/025020.
[60] B. Gertjerenken, Phys. Rev. A 88 (2013) 053623, https://doi.org/10.1103/PhysRevA.88.053623, https://link.aps.org/doi/10.1103/PhysRevA.88.053623.
[61] J.L. Helm, S.J. Rooney, C. Weiss, S.A. Gardiner, Phys. Rev. A 89 (2014) 033610, https://doi.org/10.1103/PhysRevA.89.033610, https://link.aps.org/doi/10.1103/PhysRevA.89.033610.
[62] A. Martin, J. Ruostekoski, New J. Phys. 14 (2012) 043040, https://doi.org/10.1088/1367-2630/14/4/043040, https://iopscience.iop.org/article/10.1088/1367-2630/14/4/043040/pdf.
[63] J.H. Nguyen, P. Dyke, D. Luo, B.A. Malomed, R.G. Hulet, Nat. Phys. 10 (2014) 918, https://doi.org/10.1038/nphys3135, https://www.nature.com/articles/nphys3135#citeas.
[64] L.D. Carr, R.R. Miller, D.R. Bolton, S.A. Strong, Phys. Rev. A 86 (2012) 023621, https://doi.org/10.1103/PhysRevA.86.023621, https://link.aps.org/doi/10.1103/PhysRevA.86.023621.
[65] J. Cuevas, P.G. Kevrekidis, B.A. Malomed, P. Dyke, R.G. Hulet 1210 (2013) 1681, arXiv:1210.1681, https://arxiv.org/pdf/1301.3959.pdf.
[66] H. Sakaguchi, M. Tamura, J. Phys. Soc. Jpn. 74 (2005) 292, https://doi.org/10.1103/PhysRevA.86.023621, https://link.aps.org/doi/10.1103/PhysRevA.86.023621.
[67] J. Polo, V. Ahufinger, Phys. Rev. A 88 (2013) 053628, https://doi.org/10.1103/PhysRevA.88.053628, https://link.aps.org/doi/10.1103/PhysRevA.88.053628.
[68] J.L. Helm, T.P. Billam, S.A. Gardiner, Phys. Rev. A 85 (2012) 053621, https://doi.org/10.1103/PhysRevA.85.053621, https://link.aps.org/doi/10.1103/PhysRevA.85.053621.
[69] J. Holmer, J. Marzuola, M. Zworski, Commun. Math. Phys. 274 (2007) 187, https://doi.org/10.1007/s00220-009-0871-8.
[70] B. Gertjerenken, T.P. Billam, L. Khaykovich, C. Weiss, Phys. Rev. A 86 (2012) 033608, https://doi.org/10.1103/PhysRevA.86.033608, https://link.aps.org/doi/10.1103/PhysRevA.86.033608.
[71] C. Weiss, Y. Castin, J. Phys. A, Math. Theor. 45 (2012) 455306, https://doi.org/10.1088/1751-8113/45/45/455306.
[72] A. Marchant, T. Billam, T. Wiles, M. Yu, S. Gardiner, S. Cornish, Nat. Commun. 4 (2013) 1, https://doi.org/10.1038/ncomms2893.
[73] A.M. Martin, R.G. Scott, T.M. Fromhold, Phys. Rev. A 75 (2007) 065602, https://doi.org/10.1103/PhysRevA.75.065602, https://link.aps.org/doi/10.1103/PhysRevA.75.065602.
[74] Q.-L. Cheng, W.-K. Bai, Y.-Z. Zhang, B. Xiong, T. Yang, Laser Phys. 29 (2019) 015501, https://doi.org/10.1088/1555-6611/aaea78.
[75] E. Wigner, Phys. Rev. 40 (1932) 749, https://doi.org/10.1103/PhysRev.40.749, https://link.aps.org/doi/10.1103/PhysRev.40.749.
[76] C.J. Pethick, H. Smith, Bose–Einstein Condensation in Dilute Gases, Cambridge University Press, 2003, https://physicstoday.scitation.org/doi/10.1063/1.1595060.
[77] S. Sinha, L. Santos, Phys. Rev. Lett. 99 (2007) 140406, https://doi.org/10.1103/PhysRevLett.99.140406, https://link.aps.org/doi/10.1103/PhysRevLett.99.140406.
[78] T.P. Billam, S.L. Cornish, S.A. Gardiner, Phys. Rev. A 83 (2011) 041602, https://doi.org/10.1103/PhysRevA.83.041602, https://link.aps.org/doi/10.1103/PhysRevA.83.041602.
[79] Y. Shin, M. Saba, T.A. Pasquini, W. Ketterle, D.E. Pritchard, A.E. Leanhardt, Phys. Rev. Lett. 92 (2004) 050405, https://doi.org/10.1103/PhysRevLett.92.050405, https://link.aps.org/doi/10.1103/PhysRevLett.92.050405.
[80] G.P. Agrawal, Nonlinear Fiber Optics, vol. 2, third edition, Elsevier, 2001, https://www.elsevier.com/books/nonlinear-fiber-optics/agrawal/978-0-08-047974-3.
[81] A.I. Streltsov, O.E. Alon, L.S. Cederbaum, Phys. Rev. A 80 (2009) 043616, https://doi.org/10.1103/PhysRevA.80.043616, https://link.aps.org/doi/10.1103/PhysRevA.80.043616.
[82] O.J. Wales, A. Rakonjac, T.P. Billam, J.L. Helm, S.A. Gardiner, S.L. Cornish, Commun. Phys. 3 (2020) 51, https://doi.org/10.1038/s42005-020-0320-8.
[83] A. Leanhardt, T. Pasquini, M. Saba, A. Schirotzek, Y. Shin, D. Kielpinski, D. Pritchard, W. Ketterle, Science 301 (2003) 1513, https://doi.org/10.1126/science.1088827, https://www.science.org/doi/10.1126/science.1088827.
[84] R. Gati, B. Hemmerling, J. Fölling, M. Albiez, M.K. Oberthaler, Phys. Rev. Lett. 96 (2006) 130404, https://doi.org/10.1103/PhysRevLett.96.130404, https://link.aps.org/doi/10.1103/PhysRevLett.96.130404.
[85] R. Gati, J. Esteve, B. Hemmerling, T. Ottenstein, J. Appmeier, A. Weller, M. Oberthaler, New J. Phys. 8 (2006) 189, https://doi.org/10.1088/1367-2630/8/9/189.
[86] C.R. Ooi, W.M. Liu, J. Phys. B, At. Mol. Opt. Phys. 52 (2019) 145301.
[87] R. Olf, F. Fang, G.E. Marti, A. MacRae, D.M. Stamper-Kurn, Nat. Phys. 11 (2015) 720, https://doi.org/10.1038/nphys3408.
[88] F.M. Spiegelhalder, A. Trenkwalder, D. Naik, G. Hendl, F. Schreck, R. Grimm, Phys. Rev. Lett. 103 (2009) 223203, https://doi.org/10.1103/PhysRevLett.103.223203, https://link.aps.org/doi/10.1103/PhysRevLett.103.223203.
[89] M. Mehboudi, A. Lampo, C. Charalambous, L.A. Correa, M.A. García-March, M. Lewenstein, Phys. Rev. Lett. 122 (2019) 030403, https://doi.org/10.1103/PhysRevLett.122.030403, https://link.aps.org/doi/10.1103/PhysRevLett.122.030403.
[90] D.M. Bishop, C. Pouchan, J. Chem. Phys. 80 (1984) 789, https://doi.org/10.1063/1.446789, https://aip.scitation.org/doi/10.1063/1.446789.